Influence of UDP-GlcNAc 2-Epimerase/ManNAc Kinase Mutant Proteins on Hereditary Inclusion Body Myopathy†

Juliane Penner,[‡,§] Lars R. Mantey,[‡,§] Sharona Elgavish,[§,||] Darius Ghaderi,[‡] Sebahattin Cirak,[⊥] Markus Berger,[‡] Sabine Krause,[@] Lothar Lucka,[‡] Thomas Voit,[⊥] Stella Mitrani-Rosenbaum,[#] and Stephan Hinderlich*[,‡]

Charité-Universitätsmedizin Berlin, Campus Benjamin Franklin, Institut für Biochemie und Molekularbiologie, Arnimallee 22, 14195 Berlin-Dahlem, Germany, Structural Biology Bioinformatics Unit, The Hebrew University-Hadassah Medical School, Jerusalem, Israel, Department of Pediatrics and Pediatric Neurology, University of Essen, Hufelandstrasse 55, 45122 Essen, Germany, Friedrich-Baur-Institute, Department of Neurology and Gene Center, Ludwig-Maximilians-University, Munich, Germany, and Goldyne Savad Institute of Gene Therapy, Hadassah Hebrew University Medical Center, Jerusalem, Israel

Received November 3, 2005; Revised Manuscript Received January 5, 2006

ABSTRACT: Hereditary inclusion body myopathy (HIBM), a neuromuscular disorder, is caused by mutations in UDP-*N*-acetylglucosamine 2-epimerase/*N*-acetylmannosamine kinase (GNE), the key enzyme of sialic acid biosynthesis. To date, more than 40 different mutations in the GNE gene have been reported to cause the disease. Ten of them, representing mutations in both functional domains of GNE, were recombinantly expressed in insect cells (Sf9). Each of the mutants that was analyzed displayed a reduction in the two known GNE activities, thus revealing that mutations may also influence the function of the domain not harboring them. The extent of reduction strongly differs among the point mutants, ranging from only 20% reduction found for A631T and A631V to almost 80% reduction of at least one activity in D378Y and N519S mutants and more than 80% reduction of both activities of G576E, underlined by structural changes of N519S and G576E, as observed in CD spectroscopy and gel filtration analysis, respectively. We therefore generated models of the three-dimensional structures of the epimerase and the kinase domains of GNE, based on *Escherichia coli* UDP-*N*-acetylglucosamine 2-epimerase and glucokinase, respectively, and determined the localization of the HIBM mutations within these proteins. Whereas in the kinase domain most of the mutations are localized inside the enzyme, mutations in the epimerase domain are mostly located at the protein surface. Otherwise, the different mutations result in different enzymatic activities but not in different disease phenotypes and, therefore, do not suggest a direct role of the enzymatic function of GNE in the disease mechanism.

Hereditary inclusion body myopathy (HIBM)[1] is a neuromuscular disorder characterized by adult-onset, slowly progressive distal and proximal muscle weakness, and a typical muscle pathology, including cytoplasmatic rimmed vacuoles and cytoplasmatic or nuclear filamentous inclusions composed of tubular filaments. Various hereditary forms with similar presentations have been described in diverse ethnic clusters. A recessive form of the disease, particularly common in the Jewish Persian community (with a prevalence of 1 in 1500) (*1*), presenting with an unusual feature, the sparing of the quadriceps, has been described also in other Jewish Middle Eastern population clusters (*2*) and also in non-Jewish isolated families in the Middle East (*2*) and worldwide (*3*). A single homozygous missense mutation in all Persian and other Middle Eastern Jewish and non-Jewish HIBM patients in the gene GNE, encoding the enzyme UDP-*N*-acetylglucosamine 2-epimerase/*N*-acetylmannosamine kinase (UDP-GlcNAc 2-epimerase/ManNAc kinase), was identified (*4*), confirming the founder effect hypothesis of this disorder in the Middle East. In contrast, different missense mutations in this same gene have been identified worldwide in quadriceps sparing HIBM non-Jewish patients (*4*−*8*).

GNE is the key enzyme in the biosynthetic pathway of sialic acid. Sialic acids are the most abundant terminal monosaccharides on glycoconjugates of eukaryotic cells. They comprise a family of more than 50 naturally occurring carboxylated amino sugars with a scaffold of nine carbon

† This work was supported by the Fritz-Thyssen-Stiftung, Köln, Germany (S.H. and S.M.-R.), the German-Israeli Foundation for Science Research & Development, Jerusalem, Israel (S.H. and S.M.-R.), the Association Francaise contre les Myopathies (S.M.-R.), the Mizutani Foundation for Glycoscience, Japan (S.M.-R.), the Deutsche Forschungsgemeinschaft, Bonn, Germany (L.L.; Lu 799/1-1), the Association Francaise contre les Myopathies (S.M.-R., S.C., and T.V.), and the Sonnenfeld-Stiftung, Berlin, Germany (S.H. and L.L.). S.K. receives a scholarship from The Myositis Association, Washington, DC.

* To whom correspondence should be addressed: Charité-Universitätsmedizin Berlin, Campus Benjamin Franklin, Institut für Biochemie und Molekularbiologie, Arnimallee 22, 14195 Berlin-Dahlem, Germany. Phone: +49-30-8445-1547. Fax: +49-30-8445-1541. E-mail: stephan.hinderlich@charite.de.

‡ Charité-Universitätsmedizin Berlin.

§ These authors contributed equally to this work.

|| The Hebrew University-Hadassah Medical School.

⊥ University of Essen.

@ Ludwig-Maximilians-University.

Hadassah Hebrew University Medical Center.

[1] Abbreviations: GlcNAc, *N*-acetylglucosamine; GNE, UDP-*N*-acetylglucosamine 2-epimerase/*N*-acetylmannosamine kinase; HIBM, hereditary inclusion body myopathy; ManNAc, *N*-acetylmannosamine.

10.1021/bi0522504 CCC: $33.50
Published on Web 02/10/2006

Table 1: Mutagenesis Primers for Generation of Point Mutants in the GNE cDNA[a]

Mutant	Primer
I200F	GAACAAAGAC TACATGAGCT TCATTCGCAT GTGGCTAG
C303V	GGGAACAGCA GCGTTGGGGT TCGAGAAGTT G
C303X	GGAACAGCAG CTGAGGGGTT CGAGAAG
D378Y	GAAGTTTCTC AAATCTATCT ATCTTCAAGA GCCACTGC
N519S	GTAGACAATG ATGGCAGCTG TGCTGCCCTG
F528C	GGCGGAAAGG AAATGTGGCC AAGGAAAGG
G576E	GTTGTGTCTC TGGATGAGCC TGATTGTTCC TGTGG
I587T	GAAGCCATGG GTGCACTGAA GCATACGCCT
A631T	CCATCTCATC CAAGCTACGA AACTTGGCAA TGC
A631V	CCATCTCATC CAAGCTGTGA AACTTGGCAA TGC

[a] Primers were used for QuickChange site-directed mutagenesis as described in Materials and Methods. Nucleotides different from the wild-type sequence are underlined. Only forward primers are listed; for the experiments, the respective reverse-complementary primers were also used.

atoms (*9*). Sialic acids influence adhesion processes which play an important role in many cellular functions, such as cell migration, transformation of tissues, inflammation, wound healing, and metastasis (*10*, *11*). The first step of sialic acid biosynthesis is the formation of ManNAc from UDP-GlcNAc with the simultaneous release of UDP. ManNAc is then phosphorylated by a specific kinase. These two steps are synthesized by the bifunctional enzyme GNE (*12*), which is highly conserved among mammalian species (*13*, *14*). In the following steps, sialic acid is formed by condensation of ManNAc-6-phosphate and phosphoenolpyruvate and activated by CTP to form CMP-sialic acid (*15*). This nucleotide sugar is finally used as a substrate of sialyltransferases in glycoconjugate biosynthesis (*16*).

GNE consists of two functional domains, an UDP-GlcNAc 2-epimerase domain and a ManNAc kinase domain (*17*). These two domains can be expressed separately, but a strong intramolecular dependency of the two domains has arisen during the evolution of the enzyme (*18*). HIBM patients display mutations spreading over the whole enzyme, including both domains. The mutations are composed homozygously as well as heterozygously in the patients (*4*). Although the role of GNE has been thoroughly recognized as a key enzyme in the biosynthetic pathway of sialic acid (*19*, *20*), the process by which HIBM mutations in the enzyme lead to the disease is not understood. Here we report the biochemical properties of different mutations found in non-Jewish HIBM patients. The mutations cause a reduction of both enzyme activities to different extents, in a manner independent of their localization within the GNE molecule. Furthermore, we generated models of the three-dimensional structure of both domains of GNE separately, giving insights into possible structural and interactive effects of the different mutations.

MATERIALS AND METHODS

Generation of cDNAs by Site-Directed Mutagenesis. Mutants of GNE were made by introducing point mutations, using the QuickChange site-directed mutagenesis kit (Stratagene). cDNA of human GNE, cloned into the pFastBacHTA vector (*21*), was used as template DNA. Primers used for mutagenesis are listed in Table 1. Temperature cycling amplification was performed with *PfuTurbo* DNA polymerase (Stratagene). Parental template DNA was then digested with *Dpn*I. The synthesized plasmids containing the desired mutation were transformed into supercompetent InvαF′ *Escherichia coli* cells (Invitrogen). All constructs were verified via sequencing of the whole GNE gene.

Expression of GNE Proteins in Insect Cells. Generation of baculovirus and protein expression in Sf9 cells was done by the BAC-TO-BAC system (GibcoBRL) as described previously (*21*). Briefly, pFastBac vectors were transformed into *E. coli* DH10 BAC cells. Bacmid DNA was generated by homologous recombination in the DH10 cells and isolated, and Sf9 cells were transfected with the DNA. After the first virus had been harvested, it was amplified twice and the virus titer after the last amplification step was determined. For protein expression, 2×10^6 cells/mL were infected by the viruses with a MOI of 1 and incubated for 48 h. For expression of C303X and G576E, a MOI of 3 was used and the cells were incubated for 72 h. Finally, cells were harvested, washed once with PBS, and used for protein preparation.

Purification of Proteins from Insect Cells. For protein purification, cells were resuspended in 10 mM sodium phosphate (pH 7.5), 1 mM EDTA, 1 mM dithiothreitol, and 1 mM phenylmethanesulfonyl fluoride and lysed by 20 strokes through a syringe with a narrow needle (diameter of 0.45 mm). The lysate was centrifuged at 20000*g* for 20 min, and the supernatant was applied to a Ni−NTA column (0.5 mL, Qiagen). The column was washed with 5 mL of 10 mM NaH_2PO_4, 300 mM NaCl, 0.1 mM EDTA, 1 mM dithiothreitol, and 20 mM imidazole (pH 8.0), and proteins were eluted with 2 mL of 10 mM NaH_2PO_4, 300 mM NaCl, 0.1 mM EDTA, 1 mM dithiothreitol, and 100 mM imidazole (pH 8.0). Fractions containing protein were applied to a PD-10 gel filtration column (Amersham) and eluted with 10 mM NaH_2PO_4 (pH 7.5), 100 mM NaCl, 1 mM EDTA, 1 mM dithiothreitol, and 0.1 mM UDP. Obtained fractions were checked for protein concentration by the Coomassie protein assay kit (Bio-Rad) and for purity by SDS−PAGE using a Mini-Protean II system (Bio-Rad). All experiments described below were performed with freshly prepared proteins.

Enzyme Assays. UDP-GlcNAc 2-epimerase assays for recombinant enzymes contained 45 mM Na_2HPO_4 (pH 7.5), 10 mM $MgCl_2$, 1 mM UDP-GlcNAc, and 0.2−1 μg of protein in a final volume of 200 μL. The reaction was performed at 37 °C for 30 min and stopped by boiling the mixture for 1 min. The released ManNAc was detected by the Morgan−Elson method (*22*). In brief, 150 μL of the sample was mixed with 30 μL of 0.8 M H_2BO_3 (pH 9.1) and boiled for 3 min. Then 800 μL of a DMAB solution [1% (w/v) 4-(dimethylamino)benzaldehyde in an acetic acid/1.25% 10 N HCl mixture] was added and the mixture incubated at 37 °C for 30 min. The absorbance was read at 578 nm.

The ManNAc kinase assay contained 60 mM Tris-HCl (pH 8.1), 10 mM $MgCl_2$, 5 mM ManNAc, 10 mM ATP, 0.2 mM NADH, 2 mM phosphoenolpyruvate, 2 units of pyruvate kinase, 2 units of lactate dehydrogenase, and 0.1−0.5 μg of protein in a final volume of 200 μL. The reaction was performed for 20 min at 37 °C and stopped by addition of 800 μL of 10 mM EDTA. The decrease in the amount of NADH was monitored at 340 nm.

The overall reaction of recombinant GNE was assessed by a radiometric assay. A final volume of 200 μL contained 35 mM sodium phosphate (pH 7.5), 4 mM $MgCl_2$, 0.5 mM UDP-GlcNAc, 12.5 nCi of [^{14}C]UDP-GlcNAc, 10 mM ATP, and 0.2−1 μg of purified protein. Incubations were carried out at 37 °C for 30−60 min and stopped by addition of 300 μL of ethanol. Radiolabeled substrates were separated by descending paper chromatography as previously described (*12*) and quantified by liquid scintillation analysis. The R_f values were 0.08 for UDP-GlcNAc, 0.55 for ManNAc, and 0.17 for ManNAc-6-phosphate. The assays were adjusted to rates of conversion of UDP-GlcNAc of ∼10%.

Size Exclusion Chromatography. The oligomeric state of wild-type and mutated GNE was determined with freshly prepared protein by gel filtration on a Superdex 200 HR 10/30 column (Pharmacia). A buffer containing 10 mM sodium phosphate (pH 7.5), 1 mM EDTA, 1 mM dithiothreitol, and 100 mM NaCl was used as an eluent at a flow rate of 0.2 mL/min. The column was calibrated with a protein mixture of thyroglobulin (670 kDa), γ-globulin (158 kDa), ovalbumin (44 kDa), and cytochrome *c* (17 kDa).

CD Spectroscopy. Purified proteins were transferred to CD buffer [2 mM Na_2HPO_4 (pH 7.5) and 0.1 mM DTT] by using a PD-10 gel filtration column. The protein concentration was determined by measurement of the optical density at 280 nm. A molar absorption coefficient (ϵ_{280}) of 46 935 M^{-1} cm^{-1} was predicted using the equation published by Pace et al. (*23*). Concentrations of the proteins in the experiments were 1−2 μM. CD spectra were recorded at 10 °C in a 1 mm quartz cuvette in the range of 190−260 nm on a Jasco J-720 spectropolarimeter equipped with a temperature control unit (Lauda, Königshofen, Germany). The secondary structures of the proteins were assessed using CDPro (*24*, *25*) based on 43 reference spectra of the soluble protein, named in the software as SP43. As results, the average secondary structure predictions of the CDsstr, Selcon, and Contin/LL algorithms are given.

Modeling Studies. The three-dimensional models of UDP-GlcNAc 2-epimerase and ManNAc kinase domains of GNE were based on the structures of UDP-GlcNAc 2-epimerase from *E. coli* (PDB entry 1F6D) (*26*) and the structure of glucokinase from *E. coli* (PDB entry 1Q18) (*27*) using Modeler (Accelrys Software Inc., San Diego, CA). These structures were chosen as templates for the model building since they were highly scored by the threading servers GenTHREADER (*28*, *29*) and 3DPSSM (*30*). The alignment that was generated by the GenTHREADER server was used for building the model of ManNAc kinase. The alignment for the model building of UDP-GlcNAc 2-epimerase was generated using the algorithm Align2D (Accelrys Software Inc.). The identity values of the alignments are 21 and 16% and the similarity values 40 and 34% for UDP-GlcNAc 2-epimerase and ManNAc kinase, respectively. Model building was followed by energy minimization using CHARMm (Accelrys Software Inc.). Figures of the models were generated using DS Modeling 1.1 (Accelrys Software Inc.). The glucose moiety was entered into the model of the ManNAc kinase by superimposing the model with the crystal structure of glucokinase from *E. coli* complexed with glucose (PDB entry 1SZ2) (*27*).

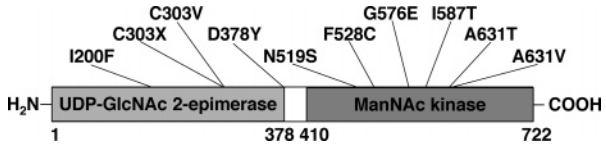

FIGURE 1: Schematic overview of GNE domain structure and localization of the HIBM mutants investigated in this study. The UDP-GlcNAc 2-epimerase domain and ManNAc kinase domain were defined by similarities between their sequences and those of related enzymes (*17*).

RESULTS

Functional Expression of GNE Proteins in Insect (Sf9) Cells. To date, more than 40 different mutations of GNE were found which cause HIBM. From these mutations, we chose 10 for biochemical analysis (Figure 1). Four of the mutations are located in the UDP-GlcNAc 2-epimerase domain of GNE, and the other six are within the ManNAc kinase domain. The mutations span a large part of the GNE protein, therefore potentially affecting different functions, including the two activities of the bifunctional enzyme. They also display different changes in amino acids, ranging from the exchange of a large side chain against a smaller one as in I587T to the introduction of a new side chain in G576E or a truncation of the GNE protein as caused by the C303X mutation. Besides N519S and I587T, all other mutations occur heterozygously in patients. In these cases, both mutations were investigated.

All mutations were introduced by site-directed mutagenesis into wild-type cDNA of human GNE, and baculovirus was generated for protein expression in Sf9 cells. Wild-type GNE and all mutants were expressed as the expected 80 kDa proteins, with the exception of C303X, which resulted in a protein of 40 kDa, indicating that the introduced stop codon is functional (data not shown). The expression levels of mutants C303X and G576E were drastically reduced. They did not exceed 1% of the total amount of soluble protein, in contrast to the other expressed proteins, which account for 20−30% of the total amount of soluble protein. On the other hand, large amounts of C303X and G576E proteins were found in the insoluble fraction after cell lysis and centrifugation. These observations have been noted in GNE proteins with gross structural changes, as reported for example in different deletion mutants of GNE (*18*), and may indicate strong effects of the mutations on the structure of the expressed proteins. For biochemical analysis, the proteins were purified from the insect cell cytosol using a Ni−NTA affinity column, taking advantage of the fused six-His tag. SDS−PAGE revealed a purity of at least 80% for all high-yield expressing proteins and of more than 50% for C303X and G576E.

Characterization of Mutants in the UDP-GlcNAc 2-Epimerase Domain of GNE. Four different point mutations were introduced into the UDP-GlcNAc 2-epimerase domain of GNE. C303V and C303X were chosen to check a potential specific role of this amino acid in GNE function, since this amino acid was affected twice in HIBM patients. I200F and D378Y occur heterozygously in one patient (*5*), but D378Y was also found in heterozygous composition in patients with A631V, a mutation in the kinase domain of GNE, which was also analyzed in this study. First, for all samples, the specific enzymatic activities of UDP-GlcNAc 2-epimerase

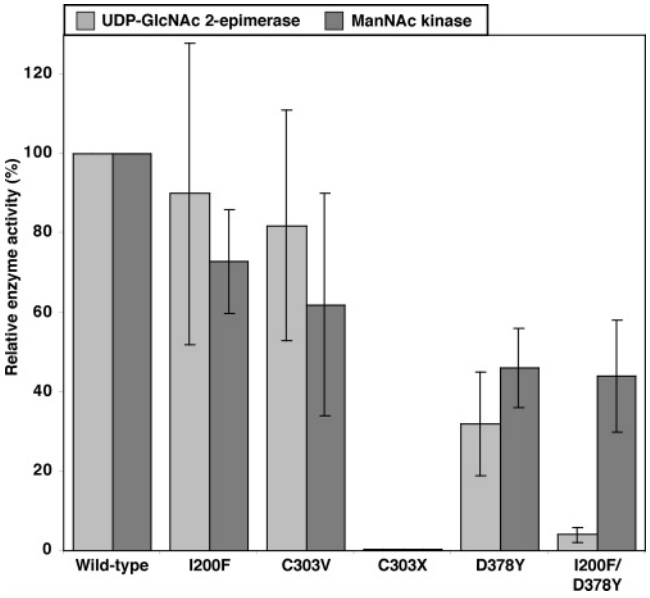

FIGURE 2: Enzymatic activities of HIBM mutants in the UDP-GlcNAc 2-epimerase domain. Proteins were expressed in Sf9 cells, affinity purified by Ni−NTA chromatography, and assayed for UDP-GlcNAc 2-epimerase and ManNAc kinase activities as described in Materials and Methods. Values are given as relative specific enzyme activities compared to that of wild-type GNE and represent means ± the standard deviation of four independent experiments.

and ManNAc kinase were determined by colorimetric assays (Figure 2). The C303X protein does not display any enzymatic activity, in agreement with the finding that the first 302 amino acids of GNE do not even cover the whole epimerase domain (*18*), and therefore, the protein is not able to form a functional enzyme. Although the I200F and C303V mutations are located within the epimerase domain, both mutants exhibited almost no reduction in epimerase activity and an only slight reduction in kinase activity. In contrast, for D378Y, a 60% reduction of epimerase activity and a 50% reduction of kinase activity were found.

Since the I200F mutation exhibited an only slight effect in particular on the epimerase activity, a double mutant of I200F and D378Y was generated next, to clarify if there is an effect of I200F on the functionality of the epimerase domain at all. The I200F/D378Y mutant displayed an epimerase activity close to the detection limit (Figure 2), indicating that the two mutations have a synergistic effect on the epimerase activity compared to each single mutation. Nevertheless, the double mutant does not represent the situation in HIBM patients, where the two mutations are located on two different alleles. No total loss of epimerase activity is therefore expected in cells of patients who were heterozygous for I200F and D378Y. The kinase activity of the double mutant was reduced to the same extent observed for the D378Y mutation alone. This suggests that this mutation is mainly responsible for the reduced kinase activity, in agreement with the localization of D378 close to the kinase domain within the primary structure of GNE (Figure 1).

It should be noted that all point mutants in the epimerase domain displayed activities lower than the activity of the wild-type enzyme, indicating that the mutations do not cause hyperactive enzymes, as observed for the R263L, R266Q,

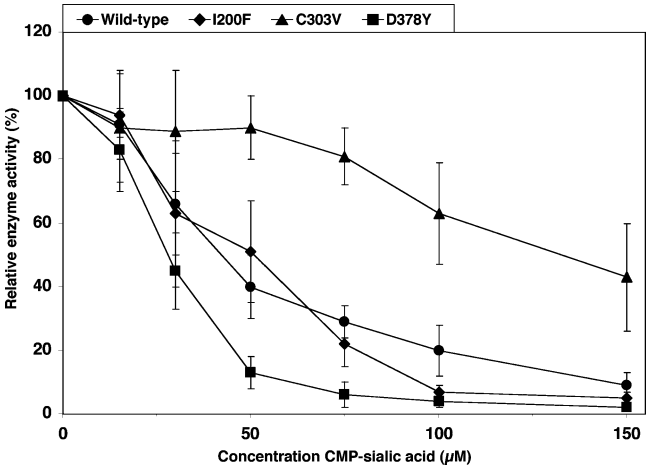

FIGURE 3: Inhibition of wild-type GNE and HIBM mutants in the UDP-GlcNAc 2-epimerase domain by CMP-sialic acid. Purified enzymes were incubated with different concentrations of CMP-sialic acid and assayed for UDP-GlcNAc 2-epimerase activity. Values are means ± the standard deviation of four independent determinations.

and R266W mutations, which result in sialuria, an additional disease caused by mutations in the GNE gene (*31*). The typical feature of sialuria is the loss of feedback inhibition of UDP-GlcNAc 2-epimerase by CMP-sialic acid, the final product of sialic acid biosynthesis. We therefore investigated the inhibition pattern of the epimerase activity of the HIBM mutants by CMP-sialic acid (Figure 3). For I200F, the concentration-dependent inhibition of epimerase activity was comparable to that of wild-type GNE. D378Y seemed to be slightly more sensitive to the feedback inhibitor at 75 and 100 μM, but the effect was not significant, because at 150 μM CMP-sialic acid all three enzymes (wild-type, I200F, and D378Y) are almost completely inhibited. For the double mutant I200F/D378Y, no results for further inhibition were obtained due to the already low epimerase activity of this mutant. Surprisingly, although C303V displays the same activity as the wild-type enzyme and the I200F mutant in the epimerase assay performed in the absence of CMP-sialic acid (see Figure 2), it is less sensitive to CMP-sialic acid inhibition than the other investigated mutant enzymes; at 150 μM epimerase, activity is reduced only 50%. This is similar to GNE enzymes carrying sialuria mutations (*31*) and is likely due to the localization of C303 close to the postulated CMP-sialic acid binding site between amino acids 249 and 275 (*32*). Nevertheless, it was not reported that HIBM patients expressing the C303V mutant or heterozygous carriers of the mutation (sialuria is a dominant hereditary disease) display the sialuria phenotype (*33*). Therefore, the question of whether there is an effect of the C303V mutation that is less drastic than that observed for the originally described sialuria mutants is still open, likely due to almost normal feedback inhibition at the usual intracellular CMP-sialic acid concentration of 20−40 μM, or if its effect is compensated by other yet unknown mechanisms.

Finally, structural changes of the GNE molecule by HIBM mutations were investigated by size exclusion chromatography and CD spectroscopy. As previously described (*12*), wild-type GNE assembles as a hexamer of 80 kDa subunits. For I200F, C303V, D378Y, and I200F/D378Y also, hexamers were found by gel filtration analysis (data not shown),

Table 2: Secondary Structures (%) of Wild-Type and Mutant GNE Revealed by CD Spectroscopy[a]

	α-helix	β-sheet	turn	random coil
WT	33	17	21	29
I200F	37	16	19	28
C303V	29	19	23	29
D378Y	27	23	21	29
N519S	15	31	22	32
F528C	40	13	20	27
A631V	28	20	24	28
M712T	32	19	22	27

[a] CD spectra were recorded as described in Materials and Methods, and secondary structures were calculated using the CDPro Software, based on 43 reference spectra of soluble proteins. Alterations of the secondary structure of low significance were defined as differences of 5−10% in one or more parameters and of high significance as differences of >10%.

Table 3: Overview of Relative Enzyme Activities of Recombinantly Expressed HIBM Mutants of GNE[a]

mutation	UDP-GlcNAc 2-epimerase activity (% of wild-type activity)	ManNAc kinase activity (% of wild-type activity)	ref	localization of amino acids within the GNE protein
R11W	15	40	*b*	surface
C13S	20	105	*36*	inside
H132Q	5	50	*36*	inside
D176V	20	85	*36*	surface
R177C	10	80	*36*	surface
I200F	90	75	this study	surface
C303V	80	60	this study	substrate binding pocket
C303X	0	0	this study	substrate binding pocket
V331A	15	115	*36*	surface
D378Y	10	105	*36*	surface
D378Y	30	45	this study	surface
I472T	50	5	*36*	inside
N519S	40	20	this study	substrate binding pocket
A524V	5	30	*36*	inside
F528C	70	35	this study	inside
F537I	45	60	*b*	inside
V572L	70	10	*36*	inside
G576E	15	15	this study	inside
I587T	55	35	this study	inside
A630T	80	40	*36*	inside
A631T	80	75	this study	surface
A631V	75	15	*36*	surface
A631V	70	65	this study	surface
G708S	45	5	*36*	inside
M712T	100	70	*35*	inside

[a] Enzyme activities were obtained from different studies indicated with their references. Data have been rounded to 5%. Localization of amino acids was derived from Figures 6 and 7. [b] From unpublished results of S. Krause.

indicating that there is no influence of the mutated amino acids on the oligomerization of the proteins. These data further exclude the possibility that the reduction of enzyme activity is due to altered quaternary structures caused by point mutations, as observed previously for histidine point mutants of GNE (*17*). For C303X, monomeric protein was detected, in agreement with the total loss of function of this protein. CD spectroscopy of the purified proteins was performed to investigate secondary structure alterations of the proteins. Wild-type GNE consists of ~33% α-helices, ~17% β-folds, and ~21% turns (Table 3). These data are in agreement with theoretical secondary structure predictions from the primary structure of human GNE (data not shown) and with the

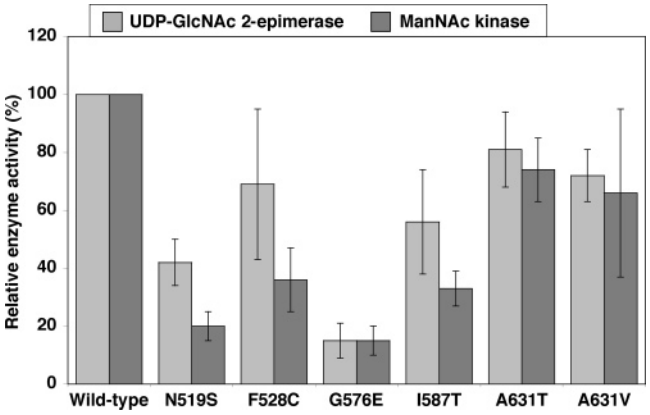

FIGURE 4: Enzymatic activities of HIBM mutants in the ManNAc kinase domain. Proteins were expressed in Sf9 cells, affinity purified by Ni−NTA chromatography, and assayed for UDP-GlcNAc 2-epimerase and ManNAc kinase activities as described in Materials and Methods. Values are given as relative specific enzyme activities compared to that of wild-type GNE and represent means ± the standard deviation of four independent experiments.

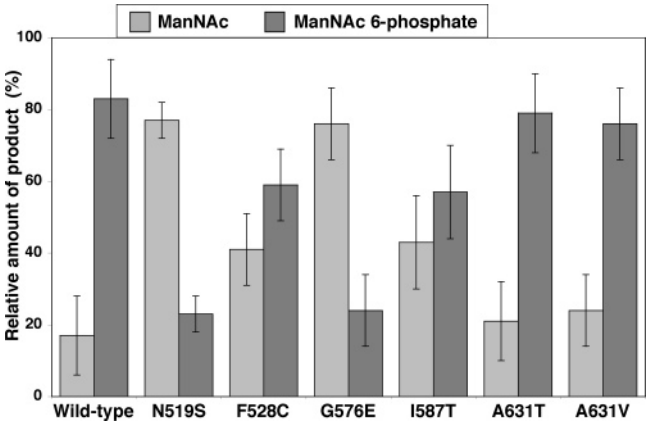

FIGURE 5: Analysis of the overall enzymatic reaction of GNE of the wild-type enzyme and HIBM mutants in the ManNAc kinase domain. Purified proteins were incubated with ^{14}C-labeled UDP-GlcNAc and unlabeled ATP, and the formation of [^{14}C]ManNAc and [^{14}C]ManNAc 6-phosphate was monitored by separation of radiolabeled compounds by paper chromatograpy as described in Materials and Methods. Values are means ± the standard deviation of three independent experiments.

models presented below (Figures 6 and 7). Whereas for C303X no CD spectra could be obtained due to the small amount of available protein, GNE carrying the I200F, C303V, and D378Y mutations displayed slight but not significant changes in the ratio of α-helices to β-folds. These data are in agreement with the almost unchanged enzyme activities of I200F and C303V and indicate that the reduced activities of D378Y are not due to secondary structure alterations.

Characterization of Mutants in the ManNAc Kinase Domain of GNE. Six HIBM mutations localized within the ManNAc kinase domain were selected for expression and characterization. Among these, the N519S mutation occurs homozygously in patients (*8*), whereas G576E and A631T mutations were identified in compound heterozygous patients (*5*). The I587T mutation was also found homozygously in Italian, American, and Gypsy patients (*5*, *34*). The A631V mutation was found homozygously as well as compound heterozygously in combination with the F528C or D378Y mutation (*5*). When expressed in insect cells, UDP-GlcNAc

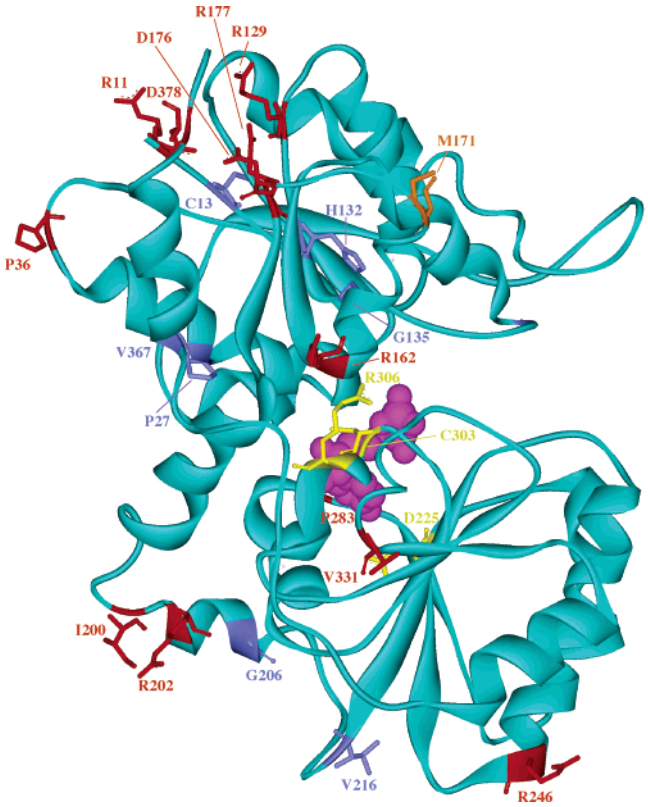

FIGURE 6: Model of the three-dimensional structure of the UDP-GlcNAc 2-epimerase domain of GNE. The model was based on the crystal structure of *E. coli* UDP-GlcNAc 2-epimerase in complex with UDP (*26*). Amino acids mutated in HIBM were highlighted and colored according to their localization with the following scheme: red for surface localization, blue for localization inside the protein, orange for those that may appear at the dimerization interface, and yellow for the substrate binding pocket.

2-epimerase and ManNAc kinase were observed with reduced activities in all these mutants (Figure 4). Whereas A631T and A631V displayed only slightly reduced activities, F528C revealed a more than 50% decreased kinase activity, whereas the epimerase activity was less affected. For N519S, the kinase activity was reduced by 80% and the epimerase activity by 60%. Despite the low yield of G576E protein after affinity chromatography, enzyme assays were still possible for this mutant. It displayed ~15% residual epimerase as well as kinase activity compared to the wild-type enzyme (Figure 4). For all mutants, inhibition of epimerase activity by CMP-sialic acid was investigated, but no difference with respect to the wild-type enzyme was observed (data not shown), suggesting an intact CMP-sialic acid binding site in all these mutant enzymes.

The specific activities of purified wild-type GNE were 1.5 units/mg for UDP-GlcNAc 2-epimerase and 2.4 units/mg for ManNAc kinase. The epimerase activity is therefore rate-limiting for the overall reaction of wild-type GNE. We developed an assay to investigate if this is also the case for GNE proteins carrying HIBM mutations. The enzymes were incubated in the presence of UDP-GlcNAc and ATP, and the formation of ManNAc as an intermediate and the formation of ManNAc-6-phosphate as the final product were detected, whereby the consumption of UDP-GlcNAc was limited to 10% to ensure constant UDP-GlcNAc 2-epimerase activity. For the wild-type enzyme, a ratio of ~1:4 of ManNAc to ManNAc-6-phosphate was found (Figure 5), indicating that under the used conditions almost all of the ManNAc released by UDP-GlcNAc 2-epimerase is immediately phosphorylated by ManNAc kinase. For A631T and A631V, the same ratios were found, whereas for I587T and F528C, the ratio of ManNAc to ManNAc 6-phosphate was ~2:3 (Figure 5), indicating that the reduced kinase activity of these mutants slightly affects the overall reaction of GNE. For N519S and G576E, the ratio of ManNAc to ManNAc 6-phosphate switched to ~4:1. For N519S, this is in agreement with the specific enzyme activities, suggesting that here ManNAc kinase is the rate-limiting enzyme and, consequently, overall flux through the sialic acid biosynthetic pathway should be reduced also in cells. For G576E, the specific ManNAc kinase activity is still higher than the specific epimerase activity. Therefore, it seems likely that ManNAc is transferred from one active site to the other within the bifunctional enzyme and that this transfer is disturbed by the mutation and consequently results in attenuated phosphorylation of the sugar. The mutants in the epimerase domain were also investigated by this assay, and the ratio of ManNAc to ManNAc 6-phosphate (~1:4) was similar to that of the wild-type enzyme for all mutants (data not shown).

The kinase mutants were also investigated by size exclusion chromatography and CD spectroscopy. N519S, F528C, A631T, and A631V were found to assemble as hexameric proteins via gel filtration analysis (data not shown). The mutations therefore do not affect oligomerization of the protein, and the observed reduced enzyme activities are due to more subtle effects. In contrast to these results, G576E assembles as a trimeric protein. The formation of trimers is in agreement with the hypothesis that the kinase domain is responsible for formation of dimeric structures (*18*), and when the dimerization site is destroyed by introduction of a glutaminyl site chain at amino acid position 576, only trimers remain. CD spectroscopy of F528C and A631V revealed only slight changes in the secondary structure of the mutated proteins (Table 2), in agreement with the weak effects on enzyme activities. The same experiment with the M712T mutation, which was characterized in more detail in a former study (*35*), confirmed that a small reduction of enzyme activities correlates with almost no alterations of the secondary structure. Only for N519S were drastic effects in CD spectroscopy found (Table 2). In comparison to the amount of the wild-type enzyme, the amount of α-helices was decreased to 15%, whereas the amount of β-folds was almost doubled. These data are in agreement with the strong effect of the N519S mutation on both activities of the enzyme.

Modeling Studies. Although localization of the HIBM mutants within the primary structure of GNE is well-defined, it is not possible to obtain a view into the three-dimensional localization of single amino acids due to the lack of a GNE crystal structure. For this reason, we generated single structural models of the epimerase and kinase domains based on related enzymes. For UDP-GlcNAc 2-epimerase, the crystal structures of three microbial homologues are known, among which the *E. coli* enzyme was highly scored by the threading servers GenTHREADER (*28*, *29*) and 3DPSSM (*30*). The threading method, which is a sequence- and structure-based method, is able to identify templates for a given sequence, even if the degree of sequence similarity is low. This is the case for *E. coli* UDP-GlcNAc 2-epimerase

and its human counterpart with a level of sequence identity of 21%. The score of the structure of *E. coli* UDP-GlcNAc 2-epimerase received for serving as a template for model building of the epimerase domain of GNE was within the range of the highest confidence level. These data strengthened our decision to use the *E. coli* enzyme as a template for the model of the human UDP-GlcNAc 2-epimerase domain of GNE.

The model of UDP-GlcNAc 2-epimerase with the UDP molecule (the crystal structure of *E. coli* UDP-GlcNAc 2-epimerase was determined in complex with a UDP molecule) is presented in Figure 6. Twenty-three amino acids known to be mutated in HIBM patients were highlighted in the model. Fourteen of them are localized at the surface of the protein, and six hydrophobic amino acids are found inside the protein. Among them, M171 is suspected to be at a potential dimerization interface, as found in the original dimeric *E. coli* UDP-GlcNAc 2-epimerase crystal structure. Three amino acids (D225, C303, and R306) are suggested to be active site amino acids, because they are localized less than 4.5 Å from the ligand. Among the 23 HIBM mutants highlighted in the epimerase model, 10 have been recombinantly expressed and analyzed for enzyme activities (Table 3). The data do not reveal significant differences between amino acids localized at the protein surface and inside the protein: almost all mutations of these amino acids reveal a relatively strong decrease in epimerase and a slight decrease in kinase activity. On the other hand, the only investigated potential active site mutant (C303V) did not reveal significant reductions in epimerase activity. Nevertheless, the fact that C303V shows activity close to that of the wild-type enzyme is not surprising. Cysteine and valine are hydrophobic amino acids with similar sizes. It therefore seems that the contribution of C303 is mainly hydrophobic, and it has no specific function in the enzymatic reaction.

The ManNAc kinase domain of GNE is a member of the sugar kinase superfamily. Therefore, we received crystal structures of several related enzymes by the threading servers. Among these, the structure of *E. coli* glucokinase (*27*) received a score at the range of the highest confidence level by GenTHREADER. It is therefore suited to serving as a template for model building of the ManNAc kinase domain of GNE, although the sequences of these proteins are only 17% identical. Very recently, a new structure of *E. coli* putative ManNAc kinase was published (PDB entry 2AA4). This structure was also highly scored by the GenTHREADER server for serving as a template for model building of the kinase domain of GNE. Its level of sequence similarity to human ManNAc kinase domain is 27%. The putative *E. coli* ManNAc kinase furthermore shows a level of sequence identity of 18% with the *E. coli* glucokinase. It seems that despite the low level of sequence identity the two proteins share a similar structure, which may also be common to the GNE kinase domain. We generated models of this kinase domain based on the structures of the *E. coli* glucokinase and putative ManNAc kinase, and a comparison of the two model structures revealed a high degree of similarity (data not shown). Furthermore, all amino acids relevant to this study are located identically. We then decided to use the *E. coli* glucokinase as a template for the final model, because its structure was also determined while it was cocrystallized with glucose (PDB entry 1SZ2), and by superimposing the model with the cocrystallized structure, we could estimate the location of the active site of the enzyme.

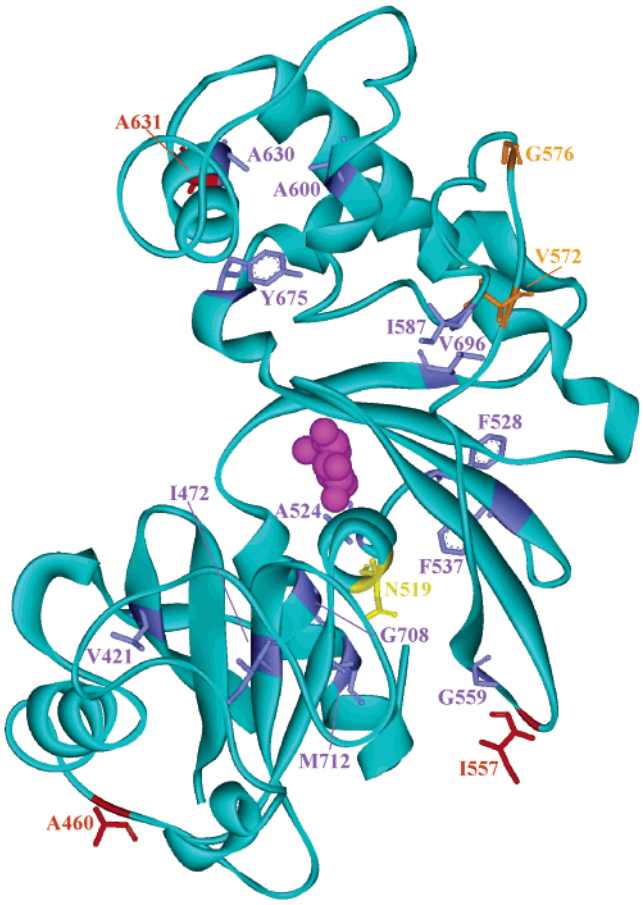

FIGURE 7: Model of the three-dimensional structure of the ManNAc kinase domain of GNE. The model was based on the crystal structure of *E. coli* glucokinase in complex with glucose (*27*). Amino acids mutated in HIBM were highlighted and colored according to their localization with the following scheme: red for surface localization, blue for localization inside the protein, orange for those that may appear at the dimerization interface, and yellow for the substrate binding pocket.

The ManNAc kinase model (Figure 7) revealed that the majority of the highlighted HIBM mutants (15 of 19) affect hydrophobic amino acids, which are located inside the protein, and only three amino acids were found at the protein surface. Amino acids V572 and G576 may be parts of a dimerization interface, which could be analogous to the dimerization site of the original *E. coli* glucokinase. Finally, N519 is localized close to the glucose molecule in the substrate binding pocket and can therefore be assigned as an active site amino acid. Enzyme activities of N519S are in agreement with this localization, because this mutant reveals reduction of kinase activity by 80%. On the other hand, localization of the other amino acids does not obviously explain differences in enzyme activities observed for the respective mutants (Table 3), and this therefore suggests more subtle effects on enzyme structure.

DISCUSSION

HIBM is a neuromuscular disease caused by mutations in GNE. Mutants of the UDP-GlcNAc 2-epimerase domain as well as of the ManNAc kinase domain of GNE were

investigated in this study for their biochemical features to gain a potential clue about the mechanism of the disease. The mutated proteins were expressed at high yields in insect cells and purified to almost homogeneity before analysis. Both specific activities of the bifunctional enzyme were reduced in each mutant, with the exception of the C303X truncated mutant, which is totally inactive. HIBM can therefore be assigned as a disease with a hypoactive GNE enzyme. Interestingly, the mutation of an amino acid in one domain of GNE also reduced the activity of the nonmutated domain. These results are in agreement with recent findings from the expression of the separated domains of GNE, which showed that both domains have a strong level of mutual adaptation (*18*). This fact also explains that, for example, in I200F and C303V the kinase domain was even more strongly affected by the mutation than the epimerase domain, where the mutation is localized. As revealed by size exclusion chromatography analysis and CD spectroscopy, most of the point mutations cause no or only subtle alterations in GNE structure, in agreement with minor effects on enzyme activity. However, mutation of N519 to serine and mutation of G576 to glutamate cause drastic structural changes in the mutants compared to the wild-type enzyme. For G576E, the effect could not be explained by the model of a monomeric protein presented in Figure 7. Interestingly, *E. coli* glucokinase and putative ManNAc kinase appear as dimers, with a very similar dimerization mode. If GNE has the same dimeric orientation as that in these two enzymes, G576 is positioned at the interface (data not shown) and may contribute to the stabilization of the dimer. Replacing the highly flexible glycine with the large and charged glutaminyl side chain may destabilize the dimer interface and results in the loss of the hexameric structure of GNE. For N519S, the model of the kinase domain (Figure 7) reveals that the amino acid is localized within an α-helix, in agreement with the loss of α-helical structures of the mutant via CD spectroscopy (Table 2). Although for this mutation a hexameric state by gel filtration analysis was detected, it is likely that the quaternary structure is changed, e.g., by wrong subunit assembly, causing the drastic reduction of enzyme activity by allosteric effects. The kinase model also displays localization of most of the mutants inside the GNE protein. It is therefore likely that a change in the folding or stability of the protein is involved in the disease mechanism. The predominant localization of the epimerase HIBM mutants on the protein surface furthermore suggests that the amino acids may be involved in the subunit interaction of GNE, resulting in an altered orientation of the subunits and a reduction of allosteric effects, or in interaction of GNE with presently unknown proteins. These interactions may also be disturbed by allosteric effects of the kinase HIBM mutants on the epimerase domain, which are underlined by the effects of the kinase mutants on epimerase activity. As a consequence, this hypothesis includes the assumption that the enzymatic activities of GNE are not involved in the pathogenic mechanism of HIBM.

Our findings on the biochemical features of the HIBM mutants are in agreement with a recent study by Noguchi et al. (*36*), which analyzed several HIBM mutants of Japanese patients by recombinant expression of the proteins in COS cells. All of the investigated mutants were also found to lead to expression of hypoactive GNE enzymes. On the other hand, in contrast of the findings in this study, the proteins expressed in COS cells predominantly assemble as trimers instead of hexamers, and a very few even form monomers, including D378Y, which was found to be hexameric in our experiments. Several reasons may explain these discrepancies. First, Noguchi et al. (*36*) analyzed the oligomeric states of the proteins by cross-linking and not by gel filtrations and did not correlate their findings directly to the functionality of the enzymes. Second, posttranslational modifications, e.g., phosphorylation or modification by O-GlcNAc as previously found for GNE (*37*), may occur specifically on GNE expressed in only one of the used systems and influence the oligomeric state. In this case, the proteins produced in COS cells may represent the native state of the enzymes better than the proteins generated in insect cells. It is also possible that the subcellular localization of GNE in mammalian cells, where it is found not only in the cytosol but also in the nucleus and associated with membranes (*38*), is different than that in insect cells and influences the oligomeric state. Third, analytical ultracentrifugation of GNE revealed dynamic formation of different oligomeric states depending on GNE concentration (D. Ghaderi, unpublished results). Protein expression in COS cells yields ~100-fold lower concentrations than expression in insect cells and may therefore result in variable formation of oligomers in different systems. Also in this case, COS cells represent the native concentration of GNE in muscle cells. The three-dimensional models of the epimerase and the kinase domain did not reveal obvious localization of the mutations identified in Japanese HIBM patients at the oligomerization sites, with the exception being V572L, which may be found at the same dimerization site as G576, if the GNE kinase domain shares a similar dimeric orientation as both *E. coli* glucokinase and ManNAc kinase do. Nevertheless, the exchange of two hydrophobic amino acids maintained the hexameric state of GNE (*36*). Taken together, these observations suggest more subtle changes in the GNE structures, which may in combination with the low GNE concentration in mammalian cells cause the observed changes in oligomerization and the more drastic reduction of enzyme activities in the mutants overlapping with our study.

The hypoactivity of the HIBM mutant GNE enzymes found in this and other studies is in contrast to that of GNE mutants causing another human disease, namely, sialuria. The sialuria mutants disrupt feedback inhibition of the UDP-GlcNAc 2-epimerase activity by CMP-sialic acid, and at least by in vitro assays, a slight increase in epimerase activity was observed (*31*). This results in an extremely high level of production of sialic acids in sialuria patient cells, suggesting that in HIBM the reduced enzyme activities cause hyposialylation of cellular glycoconjugates. This hypothesis is in agreement with the fact that loss of GNE in cells results in a drastically reduced level of production of sialic acids (*19*) and, when occurring in animals, leads to embryonal lethality (*20*). It could therefore further be assumed that HIBM is caused by a reduced level of expression of sialic acids on the cell surface of muscle cells. Several studies contribute controversial data on this issue. Whereas works of our own group demonstrated that lymphocytes (*35*) and muscle cells (*39*) of Middle Eastern HIBM patients carrying the M712T mutation do not alter their overall sialic acid content, Saito et al. (*40*) and Huizing et al. (*41*) found a reduced degree of

sialylation of distinct glycosylated epitopes of muscle tissues of HIBM patients carrying different mutations. Furthermore, Noguchi et al. (*36*) even found a reduced overall level of sialylation of muscle biopsies of Japanese HIBM patients. These effects may be due to the different impacts of the mutations on enzymatic acitivites. Whereas the M712T mutation results in only very little reduction of the UDP-GlcNAc 2-epimerase activity in cells (*35*, *39*), cells expressing mutations other than M712T, and in particular mutations affecting the epimerase domain of the enzyme, reveal a more drastic reduction in epimerase activity (*39*). It can therefore be concluded that the nature of the mutation may influence the expression of cell surface sialic acids in cells of patients. Since in all HIBM patients the same phenotype of the disease was found, differences in the age of onset or in the progression of the disease are most likely due to individual variations and are independent of the nature of the mutation, as almost all kinds of severeness have been described for example among Middle Eastern patients carrying the same M712T homozygous mutation. Furthermore, even in the studies reporting alterations in the sialylation of cells of patients, this pattern was not found in all individuals that were investigated (*36*, *40*). We therefore conclude that HIBM mutations in GNE cause reduced functionality of the enzyme and may result in a reduced level of sialylation of distinct glycoconjugates under certain circumstances, but obviously, these alterations are tolerated by muscle or other affected cells and are not the primary cause of HIBM.

ACKNOWLEDGMENT

We thank Hanns Lochmüller for fruitful discussion and Christiane Kilian for insect cell culture.

REFERENCES

1. Argov, Z., and Yarom, R. (1984) “Rimmed vacuole myopathy” sparing the quadriceps. A unique disorder in Iranian Jews, *J. Neurol. Sci. 64*, 33−43.
2. Sivakumar, K., and Dalakas, M. C. (1996) The spectrum of familial inclusion body myopathies in 13 families and a description of a quadriceps-sparing phenotype in non-Iranian Jews, *Neurology 47*, 977−984.
3. Argov, Z., Eisenberg, I., and Mitrani-Rosenbaum, S. (1998) Genetics of inclusion body myopathies, *Curr. Opin. Rheumatol. 10*, 543−547.
4. Eisenberg, I., Avidan, N., Potikha, T., Hochner, H., Chen, M., Olender, T., Barash, M., Shemesh, M., Sadeh, M., Grabov-Nardini, G., Shmilevich, I., Friedmann, A., Karpati, G., Bradley, W. G., Baumbach, L., Lancet, D., Asher, E. B., Beckmann, J. S., Argov, Z., and Mitrani-Rosenbaum, S. (2001) The UDP-*N*-acetylglucosamine 2-epimerase/*N*-acetylmannosamine kinase gene is mutated in recessive hereditary inclusion body myopathy, *Nat. Genet. 29*, 83−87.
5. Eisenberg, I., Grabov-Nardini, G., Hochner, H., Korner, M., Sadeh, M., Bertorini, T., Bushby, K., Castellan, C., Felice, K., Mendell, J., Merlini, L., Shilling, C., Wirguin, I., Argov, Z., and Mitrani-Rosenbaum, S. (2002) Mutations spectrum of GNE in hereditary inclusion body myopathy sparing the quadriceps, *Hum. Mutat. 21*, 99−105.
6. Nishino, I., Noguchi, S., Murayama, K., Driss, A., Sugie, K., Oya, Y., Nagata, T., Chida, K., Takahashi, T., Takusa, Y., Ohi, T., Nishimiya, J., Sunohara, N., Ciafaloni, E., Kawai, M., Aoki, M., and Nonaka, I. (2002) Distal myopathy with rimmed vacuoles is allelic to hereditary inclusion body myopathy, *Neurology 59*, 1689−1693.
7. Tomimitsu, H., Shimizu, J., Ishikawa, K., Ohkoshi, N., Kanazawa, I., and Mizusawa, H. (2004) Distal myopathy with rimmed vacuoles (DMRV): New GNE mutations and splice variant, *Neurology 62*, 1607−1610.
8. Broccolini, A., Ricci, E., Cassandrini, D., Gliubizzi, C., Bruno, C., Tonoli, E., Silvestri, G., Pescatori, M., Rodolico, C., Sinicropi, S., Servidei, S., Zara, F., Minetti, C., Tonali, P. A., and Mirabella, M. (2004) Novel GNE mutations in Italian families with autosomal recessive hereditary inclusion-body myopathy, *Hum. Mutat. 23*, 632.
9. Schauer, R. (2004) Sialic acids: Fascinating sugars in higher animals and man, *Zoology 107*, 49−64.
10. Hynes, R. O., and Lander, A. D. (1992) Contact and adhesive specificities in the associations, migrations, and targeting of cells and axons, *Cell 68*, 303−322.
11. Edelman, G. M., and Crossin, K. L. (1991) Cell adhesion molecules: Implications for a molecular histology, *Annu. Rev. Biochem. 60*, 155−190.
12. Hinderlich, S., Stäsche, R., Zeitler, R., and Reutter, W. (1997) A bifunctional enzyme catalyzes the first two steps in *N*-acetylneuraminic acid biosynthesis of rat liver: Purification and characterization of UDP-*N*-acetylglucosamine 2-epimerase/*N*-acetylmannosamine kinase, *J. Biol. Chem. 272*, 24313−24318.
13. Stäsche, R., Hinderlich, S., Weise, C., Effertz, K., Lucka, L., Moormann, P., and Reutter, W. (1997) A bifunctional enzyme catalyzes the first two steps in *N*-acetylneuraminic acid biosynthesis of rat liver: Molecular cloning and functional expression of UDP-*N*-acetylglucosamine 2-epimerase/*N*-acetylmannosamine kinase, *J. Biol. Chem. 272*, 24319−24324.
14. Lucka, L., Krause, M., Danker, K., Reutter, W., and Horstkorte, R. (1999) Primary structure and expression analysis of human UDP-*N*-acetylglucosamine-2-epimerase/*N*-acetylmannosamine kinase, the bifunctional enzyme in neuraminic acid biosynthesis, *FEBS Lett. 454*, 341−344.
15. Harduin-Lepers, A., Mollicone, R., Delannoy, P., and Oriol, R. (2005) The animal sialyltransferases and sialyltransferase-related genes: A phylogenetic approach, *Glycobiology 15*, 805−817.
16. Hinderlich, S., Oetke, C., and Pawlita, M. (2005) Biochemical engineering of sialic acids, in *Handbook of Carbohydrate Engineering* (Yarema, K. J., Ed.) pp 387−406, CRC Press, Boca Raton, FL.
17. Effertz, K., Hinderlich, S., and Reutter, W. (1999) Selective loss of either the epimerase or the kinase activity of UDP-*N*-acetylglucosamine 2-epimerase/*N*-acetylmannosamine kinase due to site-directed mutagenesis based on sequence alignments, *J. Biol. Chem. 274*, 28771−28778.
18. Blume, A., Weidemann, W., Stelzl, U., Wanker, E. E., Lucka, L., Donner, P., Reutter, W., Horstkorte, R., and Hinderlich, S. (2004) Domain-specific characteristics of the bifunctional key enzyme of sialic acid biosynthesis, UDP-*N*-acetylglucosamine 2-epimerase/*N*-acetylmannosamine kinase, *Biochem. J. 384*, 599−607.
19. Keppler, O. T., Hinderlich, S., Langner, J., Schwartz-Albiez, R., Reutter, W., and Pawlita, M. (1999) UDP-GlcNAc 2-epimerase: A regulator of cell surface sialylation, *Science 284*, 1372−1376.
20. Schwarzkopf, M., Knobeloch, K.-P., Rohde, E., Hinderlich, S., Wiechens, N., Lucka, L., Horak, I., Reutter, W., and Horstkorte, R. (2002) Sialylation is essential for early development in mice, *Proc. Natl. Acad. Sci. U.S.A. 99*, 5267−5270.
21. Blume, A., Ghaderi, D., Liebich, V., Hinderlich, S., Donner, P., Reutter, W., and Lucka, L. (2004) UDP-*N*-acetylglucosamine 2-epimerase/*N*-acetylmannosamine, functionally expressed in and purified from *Escherichia coli*, yeast, and insect cells, *Protein Expression Purif. 35*, 387−396.
22. Reissig, J. L., Strominger, J. L., and Leloir, L. (1955) A modified colorimetric method for the estimation of *N*-acetylamino sugars, *J. Biol. Chem. 217*, 959−966.
23. Pace, C. N., Vajdos, F., Fee, L., Grimsley, G., and Gray, T. (1995) How to measure and predict the molar absorption coefficient of a protein, *Protein Sci. 4*, 2411−2423.
24. Sreerama, N., and Woody, R. W. (2000) Estimation of protein secondary structure from circular dichroism spectra: Comparison of CONTIN, SELCON, and CDSSTR methods with an expanded reference set, *Anal. Biochem. 287*, 252−260.
25. Sreerama, N., and Woody, R. W. (2004) On the analysis of membrane protein circular dichroism spectra, *Protein Sci. 13*, 100−112.
26. Campbell, R. E., Mosimann, S. C., Tanner, M. E., and Strynadka, N. C. (2000) The structure of UDP-*N*-acetylglucosamine 2-epimerase reveals homology to phosphoglycosyl transferases, *Biochemistry 39*, 14993−15001.

27. Lunin, V. V., Li, Y., Schrag, J. D., Iannuzzi, P., Cygler, M., and Matte, A. (2004) Crystal structures of *Escherichia coli* ATP-dependent glucokinase and its complex with glucose, *J. Bacteriol. 186*, 6915−6927.
28. Jones, D. T. (1999) GenTHREADER: An efficient and reliable protein fold recognition method for genomic sequences, *J. Mol. Biol. 287*, 797−815.
29. McGuffin, L. J., and Jones, D. T. (2003) Improvement of the GenTHREADER method for genomic fold recognition, *Bioinformatics 19*, 874−881.
30. Kelley, L. A., MacCallum, R. M., and Sternberg, M. J. E. (2000) Enhanced Genome annotation using structural profiles in the program 3D-PSSM, *J. Mol. Biol. 299*, 501−522.
31. Seppala, R., Lehto, V. P., and Gahl, W. A. (1999) Mutations in the UDP-*N*-acetylglucosamine 2-epimerase gene define the disease sialuria and the allosteric site of the enzyme, *Am. J. Hum. Genet. 64*, 1563−1569.
32. Yarema, K. J., Goon, S., and Bertozzi, C. R. (2001) Metabolic selection of glycosylation defects in human cells, *Nat. Biotechnol. 19*, 553−558.
33. Tomimitsu, H., Ishikawa, K., Shimizu, J., Ohkoshi, N., Kanazawa, I., and Mizusawa, H. (2002) Distal myopathy with rimmed vacuoles: Novel mutations in the GNE gene, *Neurology 59*, 451−454.
34. Kalaydjieva, L., Lochmüller, H., Tournev, I., Baas, F., Beres, J., Colomer, J., Guergueltcheva, V., Herrmann, R., Karcagi, V., King, R., Miyata, T., Müllner-Eidenböck, A., Okuda, T., Rasic, V. M., Santos, M., Talim, B., Vilchez, J., Walter, M., Urtizberea, A., and Merlini, L. (2005) 125th ENMC International Workshop: Neuromuscular disorders in the Roma (Gypsy) population, 23−25 April 2004, Naarden, The Netherlands, *Neuromuscular Disord. 15*, 65−71.
35. Hinderlich, S., Salama, I., Eisenberg, I., Potikha, T., Mantey, L. R., Yarema, K. J., Horstkorte, R., Argov, Z., Sadeh, M., Reutter, W., and Mitrani-Rosenbaum, S. (2004) The homozygous M712T mutation of UDP-*N*-acetylglucosamine 2-epimerase/*N*-acetylmannosamine kinase results in reduced enzyme activities but not in altered overall cellular sialylation in hereditary inclusion body myopathy, *FEBS Lett. 566*, 105−109.
36. Noguchi, S., Keira, Y., Murayama, K., Ogawa, M., Fujita, M., Kawahara, G., Oya, Y., Imazawa, M., Goto, Y., Hayashi, Y. K., Nonaka, I., and Nishino, I. (2004) Reduction of UDP-*N*-acetylglucosamine 2-epimerase/*N*-acetylmannosamine kinase activity and sialylation in distal myopathy with rimmed vacuoles, *J. Biol. Chem. 279*, 11402−11407.
37. Horstkorte, R., Nöhring, S., Danker, K., Effertz, K., Reutter, W., and Lucka, L. (2000) Protein kinase C phosphorylates and regulates UDP-*N*-acetylglucosamine-2-epimerase/*N*-acetylmannosamine kinase, *FEBS Lett. 470*, 315−318.
38. Krause, S., Hinderlich, S., Amsili, S., Horstkorte, R., Wiendl, H., Argov, Z., Mitrani-Rosenbaum, S., and Lochmüller, H. (2005) Localization of UDP-GlcNAc 2-epimerase/ManAc kinase (GNE) in the Golgi complex and the nucleus of mammalian cells, *Exp. Cell Res. 304*, 365−379.
39. Salama, I., Hinderlich, S., Shlomai, Z., Eisenberg, I., Krause, S., Yarema, K., Argov, Z., Lochmüller, H., Reutter, W., Dabby, R., Sadeh, M., Ben-Bassat, H., and Mitrani-Rosenbaum, S. (2005) No overall hyposialylation in hereditary inclusion body myopathy myoblasts carrying the homozygous M712T GNE mutation, *Biochem. Biophys. Res. Commun. 328*, 221−226.
40. Saito, F., Tomimitsu, H., Arai, K., Nakai, S., Kanda, T., Shimizu, T., Mizusawa, H., and Matsumura, K. (2004) A Japanese patient with distal myopathy with rimmed vacuoles: Missense mutations in the epimerase domain of the UDP-*N*-acetylglucosamine 2-epimerase/*N*-acetylmannosamine kinase (GNE) gene accompanied by hyposialylation of skeletal muscle glycoproteins, *Neuromuscular Disord. 14*, 158−161.
41. Huizing, M., Rakocevic, G., Sparks, S. E., Mamali, I., Shatunov, A., Goldfarb, L., Krasnewich, D., Gahl, W. A., and Dalakas, M. C. (2004) Hypoglycosylation of α-dystroglycan in patients with hereditary IBM due to GNE mutations, *Mol. Genet. Metab. 81*, 196−202.

BI0522504